

# Shake-induced order in nanosphere systems

F. Járαι-Szabó, Z. Néda<sup>a</sup>, S. Aştilean, C. Farcău, and A. Kuttesch

Babeş-Bolyai University, Department of Physics, Str. Kogălniceanu 1, RO-400084, Cluj-Napoca, Romania

Received 15 May 2006 and Received in final form 19 March 2007

Published online: 18 June 2007 – © EDP Sciences / Società Italiana di Fisica / Springer-Verlag 2007

**Abstract.** Self-assembled patterns obtained from a drying nanosphere suspension are investigated by computer simulations and simple experiments. Motivated by the earlier experimental results of Sasaki and Hane and Schöpe, we confirm that more ordered triangular lattice structures can be obtained whenever a moderate intensity random shaking is applied on the drying system. Computer simulations are realized on an improved version of a recently elaborated Burrige-Knopoff-type model. Experiments are made following the setup of Sasaki and Hane, using ultrasonic radiation as source for controlled shaking.

**PACS.** 81.16.Rf Nanoscale pattern formation – 81.07.-b Nanoscale materials and structures: fabrication and characterization

## 1 Introduction

In order to use less material, to obtain a more effective storage of information or easier access to tight and narrow spaces, modern areas of engineering need structures or devices as small as possible. Nanostructures became ideal candidates in this sense. Thanks to the efforts of nanoscientists, nowadays various nanoparticles nearly monodisperse in terms of size, shape, internal structure, and surface chemistry, can be produced through reliable and standard manufacturing processes. These nanoparticles can be nanospheres, nanotubes or colloids, and can be used as building blocks for engineering more complex structures. Human-assisted construction is however very complicated and unproductive. Designing thus technologies where the building blocks self-assemble is of primary importance. In the present paper a self-assembling system which is widely used in NanoSphere Lithography (NSL) [1–8] is studied. Inspired by the earlier experimental work of Sasaki and Hane [9] and Schöpe [10], here it is confirmed by computer simulations and independent experiments that an extra shaking mechanism imposed on the drying system is benefic for engineering structures with better practical properties.

The studied system is a monodisperse polystyrene nanosphere suspension which is dried on a previously prepared silica substrate. Self-assembly is governed by several forces: i) capillarity forces, ii) electrostatic repulsion forces between the slightly negatively charged nanospheres, iii) hard-core-type repulsion forces between the nanospheres and iv) pinning forces acting on the nanospheres. Many previous studies have shown that af-

ter the drying process is completed the nanospheres self-organize in complex patterns. The case when monolayer nanosphere patterns are obtained is of special practical importance. These monolayer structures are useful as deposition masks for NanoSphere Lithography (NSL). NSL is nowadays recognized as a powerful fabrication technique to inexpensively produce nanoparticle arrays with controlled shape, size, and interparticle spacing [5, 11].

Ideally, it is expected that the nanospheres will order in the compact triangular lattice structure (Fig. 1c). However, apart from this ideal lattice topology (desirable for most of the practical purposes), many other structures are formed. Usually the patterns present many dislocations, voids or clusters (Fig. 1a, b). Sometimes instead of the triangular symmetry, the less compact square topology is selected (Fig. 1d). A fundamental goal for further progress in NSL is the development of experimental protocols to control the interactions, and thereby the ordering of nanoparticles on the solid substrates [6, 12]. Recently [12], we proposed a Burrige-Knopoff-type model [13] for understanding the pattern formation mechanism in this system. The model proved to be successful in reproducing the observed monolayer patterns, and clarified the influence of some experimentally controllable parameters. By further improving this model it is straightforward to show that applying an extra random force on the system will result in more ordered triangular nanosphere structures. One can explain thus the interesting experimental results of Sasaki and Hane [9] and Schöpe [10], and get further evidence that our Burrige-Knopoff model works fine for describing these self-assembling phenomena.

The present paper will investigate thus by large-scale computer simulations these phenomena and present also further experimental evidence in support of Sasaki and

<sup>a</sup> e-mail: zneda@phys.ubbcluj.ro

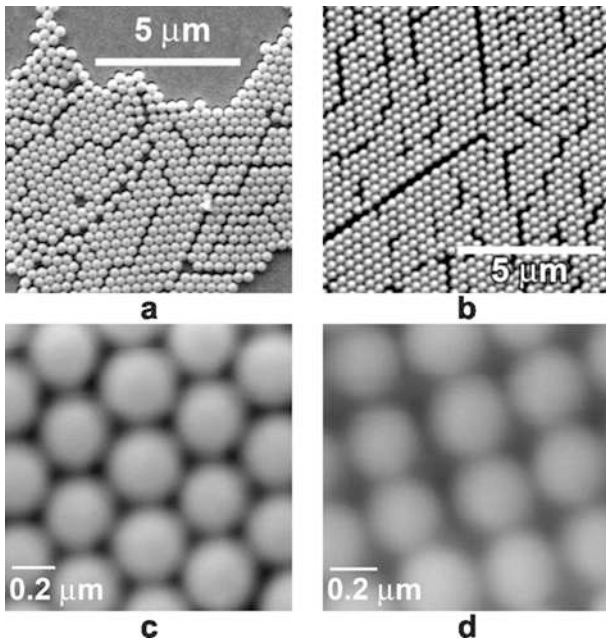


**Fig. 1.** Characteristic self-organized patterns obtained after the drying process is ended. The bottom panels illustrate the triangular and square crystallization phases. Results from our own experiments, for experimental details see [11].

Hane's and Schöpe's results. First our Burridge-Knopoff-type model [12] is presented and improved. Then simulations with an extra random or periodic shaking force are performed. Finally, as an experimental exercise the random shaking is realized by an ultrasound bath in contact with the drying nanosphere system. Both the simulations and experiments clearly confirm that the extra shaking is useful for engineering more ordered structures.

## 2 Computer simulations of the patterns

Pattern formation in the drying nanosphere suspension was recently [12] successfully modeled by a relatively simple Burridge-Knopoff-type model [13,14]. The model is rather similar to the spring-block stick-slip model used for describing fragmentation structures obtained in drying granular materials in contact with a frictional substrate [15,16]. The new feature of the model presented in [12] is that a predefined lattice structure is not imposed anymore. The model is two-dimensional; its main elements are disks which can move on a frictional substrate and springs connecting them (Fig. 2). Disks, all with the same radius  $R$ , model the nanospheres. The elastic springs reproduce the resultant of all the forces acting between the nanospheres for small separation. These forces are the lateral capillarity forces and the electrostatic repulsion between the slightly negatively charged nanospheres. Springs have similar elastic constants  $k$ , and their length is defined as the distance between the perimeters of the connected disks. There is an additional almost hard-core-type repulsion  $F_j$  which forbids disks to interpenetrate.

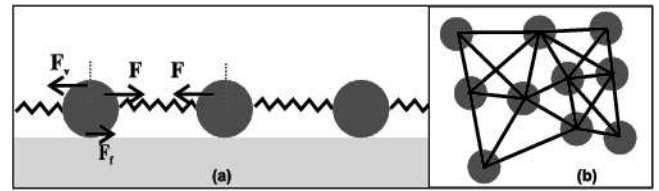


**Fig. 2.** Basic elements of the spring-block stick-slip model.

The friction (pinning) between disks and surface equilibrates a net force less than  $F_f$ . Whenever the total force acting on a disk exceeds  $F_f$ , the disk slips with an overdamped motion. The tension in each spring is proportional to the length of the spring  $F_k = kl$ , and has a breaking threshold  $F_b$ .

It is worth mentioning here that the approach based on the modified Burridge-Knopoff model seems realistic only for dense nanosphere systems where the average separation between the nanospheres is less than their radius. In this limit one can find a plausible argument for modeling the resultant forces between the nanospheres with harmonic forces. Before proceeding further with the description of the model we briefly present this argumentation.

Lateral capillarity forces have been studied in much detail both for micrometer size and nanometer size particles. Theoretical results [17–19] predict that for relatively large separation between two spheres partially immersed in a liquid one would expect an attractive force which is monotonically decaying with separation following a  $1/r$  trend ( $r$  being the distance between the centers of the two spheres). Experimental results confirm this theoretical prediction for micrometer-sized particles [20–22]. For nanometer-sized particles (our case) experiments were made only for the case when the two spheres are confined in a liquid film [23]. In this case the measured force had a non-monotonic variation with the separation of the particles. For small distances it increases almost linearly, then reaches a maximum after which it decays roughly as  $1/r$  with interparticle separation. In our case the polystyrene nanospheres are slightly negatively charged, and there is thus an additional Coulombian repulsion between them. Assuming that the lateral capillarity force decays as  $1/r$  and the Coulombian repulsion decays as  $1/r^2$ , one immediately gets that the resultant force has a non-monotonic variation and for small interparticle separation the resultant force should increase with  $r$  (Fig. 3). The easiest way to model this resultant force for small interparticle separation is by assuming a linear variation with  $r$ . This trend is also in agreement with the lateral capillarity forces measured between nanospheres confined in a liquid film [23]. The above heuristic argument is far from being complete and lacks the numerical prefactors for the strength of the Coulombian repulsion and capillarity attraction forces. It serves only as a first motivation for the application of the simple spring-block approach. In case of loose systems (where the interparticle separation is larger than the diameter of the nanospheres) one should consider also forces decaying as  $1/r$  and the relevance of the spring-block approach is questionable. It is interesting however, that even

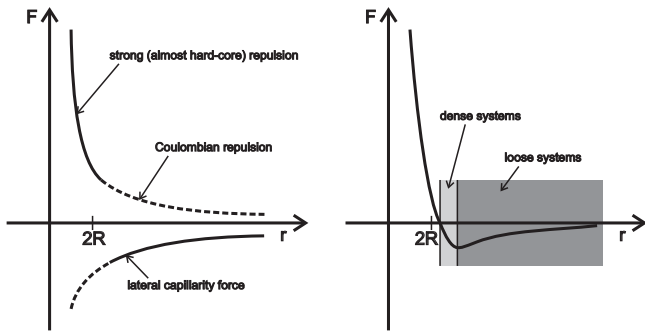


**Fig. 3.** Forces acting between the nanospheres. In the image from the right side the resultant force is plotted. Positive forces represent repulsion and negative forces attraction.

in this limit (see the pictures in [12]) the simple approach based on the Burridge-Knopoff-type model works reasonably well. In all simulations considered in the present work we will restrict ourselves to dense systems with interparticle separation much smaller than the particles' diameter. In this case the harmonic-force approach (modeling the resultant force with springs) is thus heuristically motivated and leads to realistic structures.

In the simulation, initially disks are randomly distributed and connected by a network of springs with elastic constants  $k_{ini}$  (Fig. 2b). We put springs between pairs of disks, for which the centers can be connected without intersecting another sphere (this condition will be referred to later as the geometric condition). An initially pre-stressed spring-block network is thus constructed. During each simulation step the spring constant is fixed and the system relaxes to an equilibrium configuration where the tension in each existing spring is lower than the breaking threshold  $F_b$ , and the total net force acting on each disk is lower in magnitude than the slipping threshold  $F_f$ . This relaxation is realized through several steps:

- 1) For all springs the tension  $|\mathbf{F}_k^{ij}|$  is compared with  $F_b$ . If  $|\mathbf{F}_k^{ij}| > F_b$ , the spring is broken and taken away from the system.
- 2) The total forces  $\mathbf{F}_t^i = \sum_p (d_{ip} \mathbf{F}_k^{ip} + \mathbf{F}_j^{ip})$  acting on disks are calculated (the sum is over all the other disks  $p$ ,  $d_{ip}$  is 1 if the disks are connected by a spring and 0 otherwise; the subscripts  $k$  and  $j$  denote elastic forces from springs and hard-core-type repulsion forces between disks, respectively).
- 3) Each disk is analyzed. If the magnitude of the total force  $|\mathbf{F}_t^i|$  acting on a disk is bigger than  $F_f$ , then the disk will slip with an over-damped motion governed by viscosity  $\eta$ , and its position will be changed by  $d\mathbf{r} = \mathbf{F}_t^i dt / \eta$ . The repulsive hard-core potential forbids the spheres to slide on each other and the presence of viscosity eliminates unrealistic oscillations.
- 4) During the motion of a disk it can happen that another spring is intersected. This intersected spring will break and will be taken away from the system.
- 5) After all disks have been visited in a random order and their possible motions done, the springs that fulfill the considered geometrical condition and for which

the tension is lower than the breaking threshold are redone. By this effect the rearrangement of water between nanospheres is modeled.

This concludes one relaxation step. The relaxation is continued until a relaxation step is finished without having any spring breaking or disk slipping event. After the relaxation is done, we proceed to the next simulation step and increase all spring constants by an amount  $dk$ . This step models the phenomenon that the water level of the continuous film decreases due to evaporation and the meniscus accounting for the capillarity forces gets more accentuated. The system is relaxed for the new spring constant value, and the spring constant is increased again, until all springs are broken or a stable limiting configuration is reached.

Several types of boundary conditions can be imposed. One possibility is the free boundary condition which can be realized in a simple manner by positioning initially the disks inside a circle to minimize the effect of edges. Another possibility is to consider fixed boundary conditions. This can be realized, for example, by positioning again the disks inside a circle and considering a chain of fixed disks on the chosen circle. These fixed disks are then connected with the geometrically allowed springs to other disks. One can also consider periodic boundary condition and position initially the disks inside a rectangle.

The above sequence of events can be implemented on computers and relatively big systems with over 10000 disks can be simulated in reasonable computational time. The model, as described above, has several parameters: the value of the static friction force  $F_f$ , the value of the breaking threshold  $F_b$  of springs, the initial value of spring constants  $k_{ini}$ , the spring constant increasing step  $dk$ , the value of viscosity  $\eta$ , the parameters of the Lennard-Jones potential which realizes the hard-core repulsion, the radius of disks  $R$ , and the initial density of nanospheres  $\rho = S / (N\pi R^2)$  (where  $S$  is the simulation area and  $N$  is the number of considered disks). Varying these parameters in reasonable limits all experimentally obtained patterns can be successfully modeled [12].

An immediate question that arises in connection with the approach based on the spring-block model concerns its computational efficiency. What do we gain by using this simplified force pattern instead of the more complete variation sketched on Figure 3? The answer comes from several sights. First, the exact shape of the force given in Figure 3 is undetermined since the two prefactors for the Coulombian and capillarity forces are unknown. Due to this, there would appear an extra unknown parameter which determines the shape of the resultant force, making the model more complex. Secondly, the breaking threshold imposed on the springs allows the use of a natural cutoff for the interparticle forces, and makes simulations faster. Third, the simple harmonic force allows a more rapid calculation of the resultant forces. Finally, the geometric condition imposed on springs (not to intersect another nanosphere) ensures the screening effect imposed by other nanospheres on capillarity and Coulombian forces.

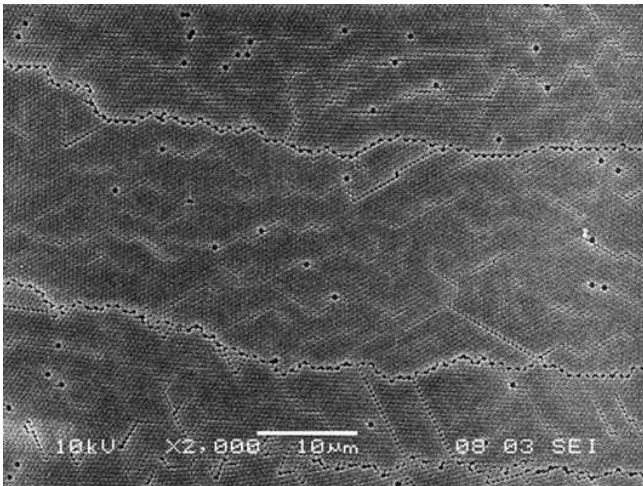


**Fig. 4.** Characteristic dried nanosphere pattern obtained experimentally after the drying front has moved in the horizontal direction.

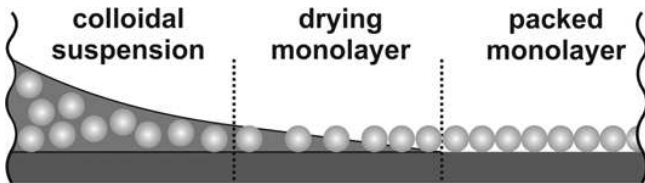


**Fig. 5.** The three different regions in the improved model.

The above-mentioned model considered a uniform decrease of the liquid level in the whole system. Experimental studies show however that this approach is not valid in real systems. During the drying process large liquid level gradients are present, leading to the flow of the nanosphere suspension from one part of the sample to another one [1,2]. In most of the experimental samples thus drying fronts can be observed separating already dried and wet parts of the sample. This non-uniform liquid level is also facilitated by almost all types of suspension deposition methods on the silica substrate. The obtained larger-scale patterns are strongly influenced by the drying front. Experiments have shown that the characteristic larger-scale fracture lines tend to be perpendicular to the direction of the drying front (Fig. 4).

Recently a simple lattice-gas-type model was proposed in order to explain the self-assembly process driven by the drying liquid front [24]. Monte Carlo simulations with the classical Metropolis algorithm proved that patterns resembling the experimentally obtained ones can be obtained by using this elegant approach.

Our model can be also further improved and made thus more realistic to incorporate the effects generated by the moving drying front. In order to do this we consider three different regions inside the simulated area (Fig. 5).

In region I the liquid level is greater than the nanosphere diameter, no capillary effects are present. This models the colloidal suspension state on the substrate (regions with excess of liquid). In this region the dynamics is governed by a hard-core repulsion between spheres and

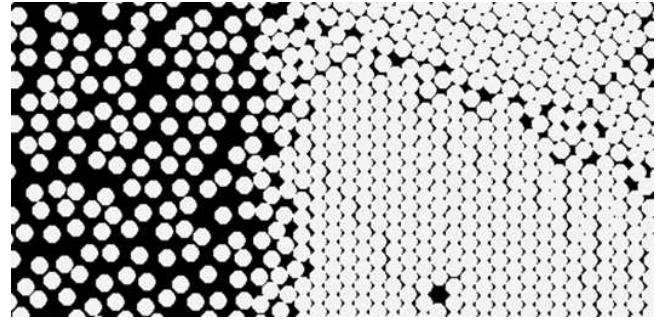


**Fig. 6.** Snapshot from simulation. On the left side one can observe the spheres in region I and spheres on the right side of the picture are already in region III. The drying front is also clearly detectable.

a constant force from left to right which results from the liquid convection (liquid is flowing from left to right). The pattern formation mechanism takes place in region II, where the liquid level is lower than the height of the nanospheres. This is the region that was considered in our earlier model. Here, the dynamics is governed by capillary effects, friction with the substrate and repulsion between disks, as described earlier. When nanospheres get in this region, they become connected with springs having elastic constants  $k_{ini}$ . Finally, the third region (III) represents the final packed monolayer structure where no more forces are acting on nanospheres. The separation line between region II and III defines the drying front in the system.

In the simulations initially we consider all nanospheres in region I, and distribute them randomly with a somehow smaller density. We define a given thickness for region II (usually  $1/3$  of the width of the simulated region), and this region slowly progresses with a constant speed from the right to the left. Region I gets thus less and less narrow and finally we end up with all spheres in region III. During simulation new particles are constantly supplied from the left and driven by the constant force in the direction of the separation line between region I and region II. A snapshot from the simulation can be observed in Figure 6 and a characteristic final pattern is shown in Figure 7. A qualitative comparison between Figure 4 and Figure 7 will convince us that this improved model works excellently and all types of defects observable in experiments are reproduced by simulation.

### 3 Effect of a random force

An extra shaking force acting on the nanospheres can be now imposed during the simulated drying process. Two types of simulations were performed, using both the original and the improved version of the spring-block model. In the original version of the spring-block model we consider an extra stochastic force acting on each nanosphere. This random force will model the influence of a random shaking applied on the drying nanosphere suspension, and it approximates reasonably well the experimental conditions of Sasaki and Hane [9], where an ultrasound bath was used to generate the shaking. Second, we consider the

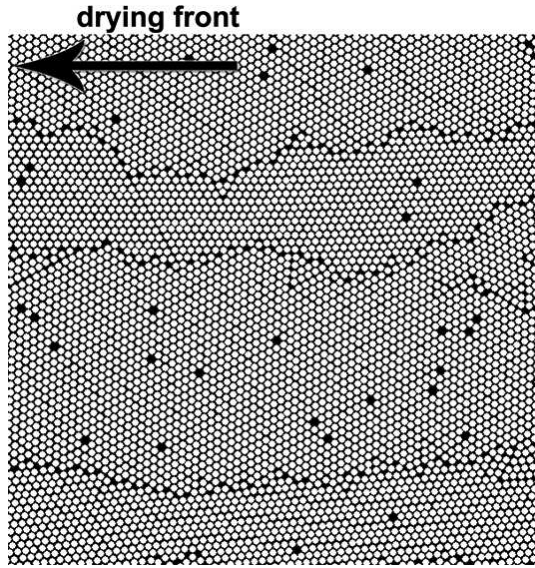


**Fig. 7.** Typical structure obtained by computer simulations with the improved (three-region) model. Simulation parameters are:  $F_f = 0.003$ ,  $F_b = 0.05$ ,  $k_{ini} = 0.01$ ,  $dk = 0.001$ ; the speed of the interface between region I and region II was chosen to be  $10^{-6} * L/steps$  ( $L$  is the total length of the simulated region and  $steps$  stands for relaxation steps in the simulation).

improved model where in region II an oscillating force is applied on each nanosphere. This force is the same for all nanospheres and acts in the direction of the drying front. This simulation corresponds to the experimental setup of Schöpe [10]. In this experiment the inclined deposition method was used for the deposition of the liquid film, and an extra oscillating electric field perpendicular to the direction of the drag was applied on the nanospheres.

### 3.1 The original model with an extra stochastic force

An extra  $F_r$  force completely uncorrelated in time and space was imposed on each nanosphere. The orientation of this force was chosen to be totally random in the simulation plane and its strength was chosen with a uniform distribution in a fixed  $F_r \in [0, F_R]$  interval. The value of  $F_R$  characterizes thus the strength of the applied random perturbation. In order to achieve a final stable configuration it is evident that the condition  $F_R \leq F_f$  must be satisfied. By fixing the other parameters of the simulations the influence of  $F_R$  was systematically studied. Fixed boundary conditions in a disk-like geometry were used and a central rectangular region was studied. Extensive simulations proved that by increasing the value of  $F_R$  ( $F_R \leq F_f$ ) more and more ordered structures are self-assembled. In Figure 8 we illustrate this trend for two different parameter sets. Simulation results confirm thus that a random shaking during the drying process could be helpful in engineering more ordered structures. The effect is reasonable, since the random force will reorder regions during the whole simulation process. Dislocations, voids or fracture lines formed in the early stages when many springs are present will disappear during the dynamics,

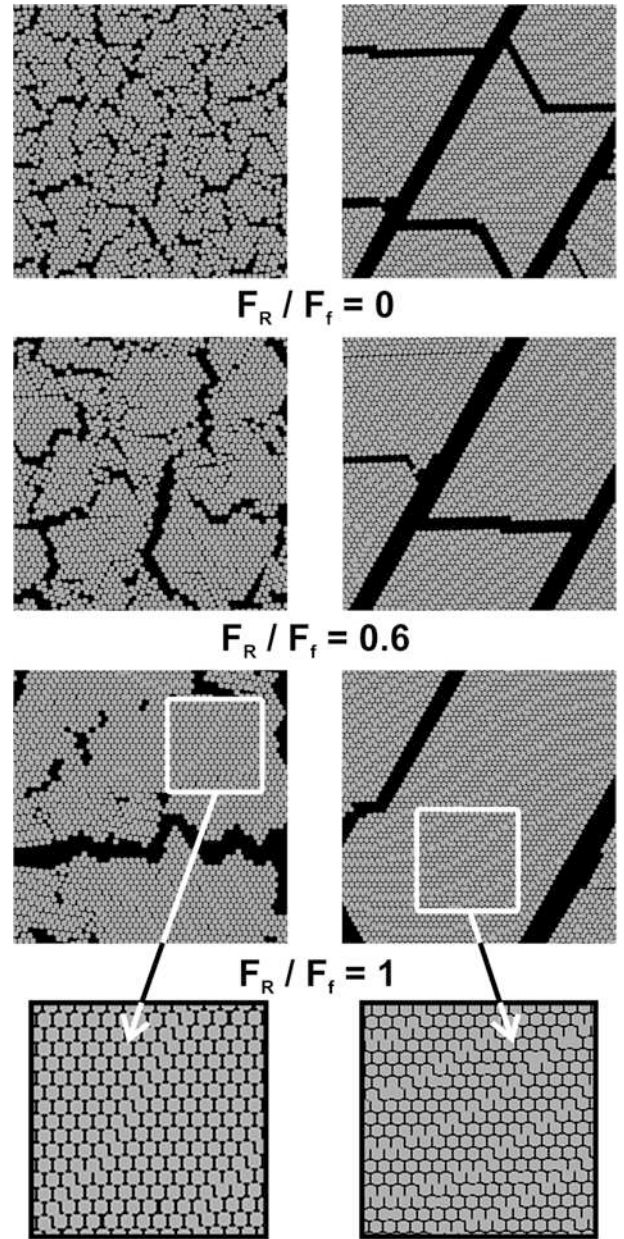


**Fig. 8.** Influence of the strength of the applied random force on the final stable patterns. Results for two different parameter sets are shown. The pictures on the left side have been obtained with  $F_b = 0.05$  and the ones on the right side with  $F_b = 0.1$ . Other parameters of both simulations are:  $F_f = 0.005$ ,  $k_{ini} = 0.01$ ,  $dk = 0.001$  and  $\rho = 0.749$ .

and the structure will evolve more homogeneously. It is also observable from Figure 8 that although larger ordered domains are generated with increasing  $F_R$  values, the fracture lines become also wider. This effect is however mainly due to the imposed fixed boundary conditions.

### 3.2 The improved model with an extra oscillating force

Within the improved model we applied an additional harmonic  $F_h = F_0 \sin(\omega t)$  force in region II. The period of

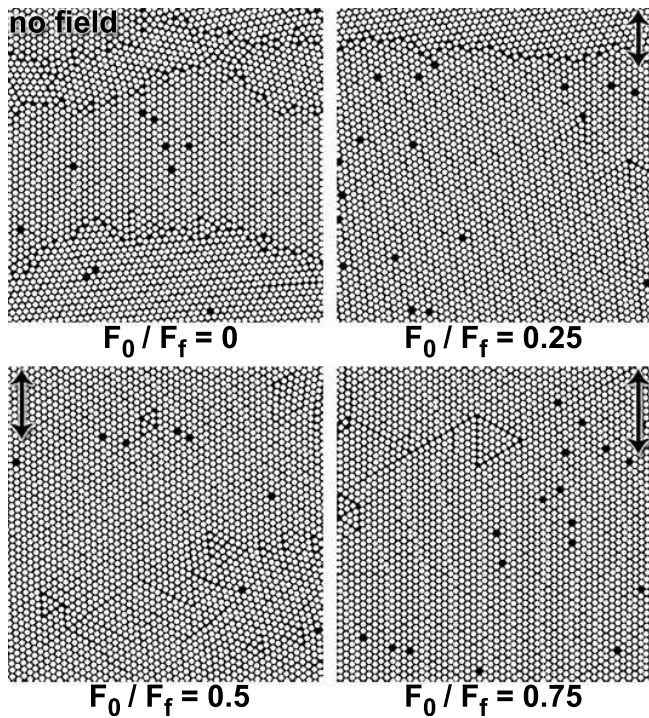


**Fig. 9.** Final patterns obtained with an extra harmonic force in region II. The successive pictures are for  $F_0 = 0, F_f/4, F_f/2$  and  $3F_f/4$  amplitude values, respectively. The other simulation parameters are as in Figure 8.

the harmonic force was chosen to be of the order of hundreds of relaxation steps. The  $F_0$  amplitude of this force was systematically varied in the  $F_0 \in [0, F_f]$  interval. The obtained results are similar to the ones obtained with a random force. Increasing the value of  $F_0$  in the  $[0, F_f)$  interval, the obtained structures become more ordered and present less defects. The result is stable and the qualitative behavior does not change whenever the parameters of the simulations are varied. A characteristic series of final patterns as a function of  $F_0$  is illustrated in Figure 9. The simulated series from Figure 9 describes well the experimental results presented in [10]. Simulations suggested also that higher frequencies eliminate more defects, although the qualitative changes in the final structures are much less evident than the results presented in Figure 9. For a systematic study on the frequency dependence, simulations with much bigger system sizes will be necessary.

## 4 Experiments

As an experimental exercise we have also reproduced the results of Sasaki and Hane [9]. Following their work the shaking was realized by an ultrasound radiation. The experimental samples were prepared following the drop-coat method [3–5]. Of critical importance for nanosphere ordering is the initial chemical treatment of the glass substrate in order to render the surface hydrophilic and improve its wettability (for details, see [12]). Polystyrene nanospheres of 400 nm diameter, exhibiting negatively

charged carboxyl-terminated surface with a strongly hydrophobic nature, were supplied as monodispersed suspensions in deionized water (wt. 4%). The original suspension of polystyrene nanospheres was diluted by 10 and a volume of  $100 \mu\text{l}$  diluted solution was evenly spread on the pre-treated substrates. As the water evaporates and the samples are dried, the nanospheres self-assemble into close-packed monolayer arrays exhibiting many fracture lines, dislocations or other types of defects.

In order to investigate the influence of the shaking effect, drying was realized in two different conditions. Six samples were studied, half of them were dried simply in the normal atmosphere of the lab while the other half was exposed to a shaking effect induced by an ultrasound bath.

We have used an Elma Transsonic 35 kHz frequency ultrasound bath filled with water. The glass plates holding the nanosphere solution was positioned on the surface of the water by using a 10 cm diameter and 0.4 cm thick cork floater with a disk-like geometry. In the middle of the floater a hole with a 0.8 cm diameter was created, allowing direct contact between the liquid from the ultrasonic bath and the surface of the glass plates. Shaking is induced thus by the acoustic vibrations transmitted through the glass plates.

In both cases (with and without ultrasound) the samples were completely dried. Drying was achieved in approximately 45 minutes for the sonicated samples. For the non-sonicated samples complete drying was achieved roughly twice slower. The microstructure of the dried samples was studied by scanning electron microscopy (SEM) using a JEOL JSM 5600 LV electronic microscope. By surveying different regions of the substrates we have qualitatively analyzed and compared the engineered nanosphere patterns.

Our experimental exercise confirms the picture suggested by Sasaki and Hane: sonicated samples shows more extended and ordered triangular lattice structures than non-sonicated ones. From a first look at a randomly selected region on a sonicated and a non-sonicated sample, this result is however not immediate. One has to remember that due to the non-homogeneous spreading of the liquid film, different regions in the same sample might exhibit different level of ordering. In order to obtain thus a clear conclusion many different regions have to be analyzed and a statistical conclusion has to be drawn. We

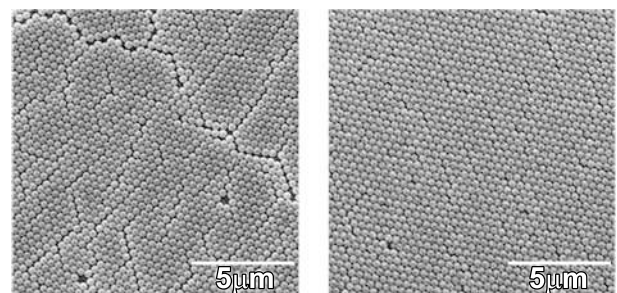


**Fig. 10.** Visual comparison between characteristic regions of non-sonicated (left) and sonicated samples (right).

have analyzed tens of different regions and qualitatively found that sonicated samples had a lower number of fracture and dislocation lines, the triangular lattice structures being more extended in this case. For visually illustrating this, in Figure 10 we present a characteristic pattern found on sonicated samples in comparison with a characteristic pattern found on non-sonicated samples.

## 5 Conclusions

Nanosphere self-assembly from a drying suspension was studied in the presence of a moderate intensity shaking. To understand this pattern formation phenomenon two models were considered, i) the simple Burrige-Knopoff-type spring-block model [12] and ii) an improved version of this model where the withdrawal of the liquid front and its effect on self-assembly are also taken into account. In both cases beside the relevant capillarity, Coulombian and friction (pinning) forces and also an extra random shaking were imposed. Computer simulations suggested a clear conclusion: a moderate intensity extra shaking imposed on the drying nanosphere system will yield more ordered final patterns. Increasing the intensity of the random force up to the limit of the pinning forces acting on the nanospheres is always beneficial and eliminates most of the defects. The simulation performed on our original spring-block model with an extra random force describes well the experimental results of Sasaki and Hane [9], while the simulations realized on the improved model with an extra directional harmonic force acting in region II correspond to the experimental setup of Schöpe [10]. In agreement with experiments computer simulations also yield that primary (larger) fracture lines are formed predominantly in the direction of the moving liquid front (for experiments see Fig. 4 and for simulations Fig. 6 or 7). The patterns and the trend obtained by computer simulations describe thus qualitatively well the experimentally obtained ones, giving new evidence for the applicability of the simple Burrige-Knopoff-type models in modeling this system.

We have not analyzed here the influence of the frequency of the shaking. The first reason for this is that the influence of the shaking frequency on the final pattern is less evident than the influence of the intensity of the shaking force. In order to get reliable data, computer simulations on much larger systems have to be done. The computing power presently available for us does not allow studying much larger systems in reasonable (months) computing time. Second, the simulations in the present form lack real time. Instead of time we used the relaxation steps for characterizing the dynamics. Relaxation steps might correspond however to different time intervals and in this sense the frequency of the imposed oscillating force has only a qualitative meaning.

As an exercise we have also repeated the experiments done by Sasaki and Hane, confirming their results. During the experiments we realized that in order to get more extended triangular lattice structures and less defects, one will have to further optimize the experimental conditions.

To make the experiments less costly, computer simulations could be useful. The present work shows that a simple Burrige-Knopoff-type model works empirically well and can be helpful to give a first estimate on the influence of many experimentally controllable parameters.

The present work has been supported by the research grant CNCSIS 41/183 and CEEEX-Nanobiospec 2006. The research of F. Járαι-Szabó has also been supported by the Fellowship Program for Transborder Hungarian Scientific Research - Hungarian Academy of Science. Discussions and helpful comments from Prof. Peter Kralchevsky are gratefully acknowledged.

## References

1. N.D. Denkov, O.D. VeleV, P.A. Kralchevsky, I.B. Ivanov, H. Yoshimura, K. Nagayama, *Langmuir* **8**, 3183 (1992).
2. N.D. Denkov, O.D. VeleV, P.A. Kralchevsky, I.B. Ivanov, H. Yoshimura, K. Nagayama, *Nature* **361**, 26 (1993).
3. Ch.L. Haynes, R.P. van Duyne, *J. Phys. Chem. B* **105**, 5599 (2001).
4. K. Kempa *et al.*, *NanoLett.* **3**, 13 (2003).
5. W.A. Murray, S. Astilean, W.L. Barnes, *Phys. Rev. B* **69**, 165407 (2004).
6. A.A. Chabanov, Y. Jun. D.J. Norris, *Appl. Phys. Lett.* **84**, 3573 (2004).
7. E. Vasco *Appl. Phys. Lett.* **85**, 3714 (2004).
8. K. Chen, A. Taflove, Y.L. Kim, V. Backman, *Appl. Phys. Lett.* **86**, 033101 (2005).
9. M. Sasaki, K. Hane, *J. Appl. Phys.* **80**, 5427 (1996).
10. H.J. Schope, *J. Phys.: Condens. Matter* **15**, L533 (2003).
11. M. Baia, L. Baia, S. Astilean, *Appl. Phys. Lett.* **88**, 143121 (2006).
12. F. Járαι-Szabó, S. Astilean, Z. Néda, *Chem. Phys. Lett.* **408**, 241 (2005).
13. R. Burrige, L. Knopoff, *Bull. Seismol. Soc. Am.* **57**, 341 (1967).
14. J.H.E. Cartwright, E. Hernandez-Garcia, O. Piro, *Phys. Rev. Lett.* **79**, 527 (1997).
15. K.-t. Leung, Z. Néda, *Phys. Rev. Lett.* **85**, 662 (2000).
16. Z. Néda, K.-t. Leung, L. Józsa, M. Ravasz, *Phys. Rev. Lett.* **88**, 095502 (2002).
17. D.Y. Chan, J.D. Henry, L.R. White, *J. Colloid Interface Sci.* **79**, 410 (1981).
18. P.A. Kralchevsky, V.N. Paunov, N.D. Denkov, I.B. Ivanov, K. Nagayama, *J. Colloid Interface Sci.* **155**, 420 (1993).
19. V.N. Paunov, P.A. Kralchevsky, N.D. Denkov, K. Nagayama, K. Nagayama, *J. Colloid Interface Sci.* **157**, 100 (1993).
20. C.D. Dushkin, P.A. Kralchevsky, H. Yoshimura, K. Nagayama, *Phys. Rev. Lett.* **75**, 3454 (1995).
21. C.D. Dushkin, P.A. Kralchevsky, V.N. Paunov, H. Yoshimura, K. Nagayama, *Langmuir* **12**, 641 (1996).
22. C.D. Dushkin, H. Yoshimura, K. Nagayama, *J. Colloid Interface Sci.* **181**, 657 (1996).
23. K.D. Danov, B. Pouligny, P.A. Kralchevsky, *Langmuir* **17**, 6599 (2001).
24. E. Rabani, D.R. Reichman, P.L. Geissler, L.E. Brus, *Nature* **426**, 271 (2003).